Chinese Chemical Letters 31 (2020) 2683–2688

Contents lists available at ScienceDirect

Chinese Chemical Letters

journal homepage: www.elsevier.com/locate/cclet

Communication

Ultrahigh flux of graphene oxide membrane modified with orientated growth of MOFs for rejection of dyes and oil-water separation

Meng Zhu[a], Yucheng Liu[a,b,*], Mingyan Chen[a,b], Dong Gan[a], Maoren Wang[a], Haojie Zeng[a], Maoqi Liao[a], Jie Chen[a], Wenwen Tu[a,*], Wen Niu[a]

[a] College of Chemistry and Chemical Engineering, Southwest Petroleum University, Chengdu 610500, China
[b] Research Institute of Industrial Hazardous Waste Disposal and Resource Utilization, Southwest Petroleum University, Chengdu 610500 China

ARTICLE INFO

Article history:
Received 2 March 2020
Accepted 17 March 2020
Available online 14 April 2020

Keywords:
GO composite membrane
Metal organic frameworks
Mg/Al-LDHs
Orientated growth
Ultra-high flux

ABSTRACT

Metal organic frameworks (MOFs) has broad application prospect in separation, catalysis, and adsorption. By a facile green method, we successfully fabricated prGO@cHKUST-1 composite membrane with the modification of dopamine and orientated growth of MOFs. Mg/Al-layered double hydroxides (Mg/Al-LDHs) was used as a modulator to obtain cubic HKUST-1 (cHKUST-1) with excellent morphology and special properties. Scanning Electron Microscopy (SEM), X-ray diffraction (XRD), and Fourier transform infrared spectroscopy (FTIR) *etc.* characterization illustrated successful synthesis of cHKUST-1 and composite membranes. Cubic HKUST-1 can tune the inter-layer spacing of graphene oxide (GO) leading increase in hydrophilicity and flux of the membrane. Meanwhile, the reduction effect of PDA and intercalation effect of MOFs could change the stacked way of GO layers, forming several fuzzy pores and more active sites on membrane surface. The prGO@cHKUST-1 membrane has an excellent rejection for methylene blue (MB) (99.5%) and Congo red (CR) (71.2%). Moreover, the modified membrane exhibited 10 and 5 times higher permeation flux than that of original GO membrane and prGO membrane, respectively. Thus, using orientated growth of MOFs to synthesize GO based composite membrane will provide useful insights in ultrahigh permeation flux membranes of dye and oil-water emulsion separation.

Environmental pollution has become a social problem. Among them, the problem of water pollution which caused by organic dyes and oils has recently been particularly prominent [1,2]. When organic dyes enter water, they may weak the photosynthesis of aquatic plants, and the oil can decrease the dissolved oxygen and thus affect ecological balance [3]. Organic dyes are carcinogenic, teratogenic and mutagenic, posing a great threat to aquatic organisms and human health. With the development of dyestuff towards the direction of anti-photodecomposition, anti-oxidation and anti-biodegradation, it is increasingly difficult to treat dyestuff wastewater with common water treatment methods [4,5]. An effective and urgent method is needed to deal with oil-water emulsion. Traditional techniques such as coalescing agents, sedimentation tanks, centrifuges, magnetic separation and flotation techniques were used to separate oily wastewater but not suitable for oil-water emulsion [6]. Thus, improved method is needed to deal with organic dye and oil-water emulsion wastewater.

Membrane materials with a micro-porous structure and adsorption capacity can continuously remove organic dye and separate oil-water emulsion [7]. However, certain membranes are hydrophobic, easily blocked and unstable which prevent its broad applications [8]. Some researchers pointed out that surface modification, hydrophilic coating and mixing with nanomaterials are effective ways to solve the above problems [9]. Grapheme oxide (GO) is a two-dimensional material, which has high specific surface area, and abundant functional groups on its surface [10,11]. Moreover, GO is widely used in the fields of analysis and detection, polymer materials, biomedicine and optoelectronic materials [12–14]. Some researchers reported that GO composite membrane can remove organic dye and separate oil-water emulsion, and it has been proved to be improved eff ;ective in water purification [15,16]. Zhang *et al.* [17] synthesized a spindle-knotted PAN/GO composite membrane with the modification of polyacrylonitrile. And this membrane exhibits excellent rejection (99%) and flux (3500 LMH) properties for oil-water separating.

* Corresponding authors at: College of Chemistry and Chemical Engineering, Southwest Petroleum University, Chengdu, 610500, China.
E-mail addresses: liuyc@swpu.edu.cn (Y. Liu), 294658430@qq.com (W. Tu).

https://doi.org/10.1016/j.cclet.2020.04.011
1001-8417/

Recently, GO and metal organic frameworks (MOFs) composite membrane has attracted widespread attention from researchers. MOFs is formed by metal ions and organic ligands which have high stability, organic functionality, large surface area, and high porosity [18]. T.A. Makhetha *et al.* [19] prepared a series of Cu(tpa)@GO/PES composite membranes with antifouling properties, and the rejection rate of Congo red (CR) is 80%. They found that MOFs can increase layer spacing of GO and adsorption capacity of the composite membrane. Layered double hydroxides (LDHs) is reported to be available and inexpensive material which widely used in medicine, catalysis and adsorption [20,21]. It was used as a modulator to control growth direction of crystal in previous study [22]. However, there are few studies on the combination of LDHs and MOFs active sites. Because of unsaturated coordination state of metal atoms on the surface of LDHs and the active sites of nucleation and directional growth, LDHs can be used as a supporting material for the orientated growth of MOFs [23]. Chakraborty *et al.* [18] synthesized MgAl-LDH/Cu-(BDC) MOFs composite for removing high concentration anionic dye, which rejection is 99%. The performance of MOFs can be optimized by modification of LDHs. For HKUST-1, the crystal shape can be changed from octahedral to cubic under the action of LDHs. Compared with other two HKUST-1, the micropore volume and surface area of cubic HKUST-1 (cHKUST-1) are 1.3 cm^3/g and 2642 m^2/g, respectively. Moreover, cHKUST-1 is more stable and alkali-tolerant [24]. In this work, cHKUST-1 was used to synthesize the prGO@cHKUST-1 composite membrane, and the organic dye rejection and oil-water emulsion separation properties were tested. With the reduction and adhesive effect of poly-dopamine (PDA), partially reduced GO (prGO) tightly coupled membrane was obtained. Properties of original GO and prGO membranes were also studied and compared.

GO was synthesized *via* the modified Hummers method. To obtained cHKUST-1, the LDHs nanosheets were prepared by an improved method [25]. With the modification of LDHs, the cHKUST-1 was synthesized by hydrothermal method. Subsequently, prGO membrane material consist of GO and dopamine was prepared. With the modification of cHKUST-1 and dopamine, the prGO@cHKUST-1 membrane material was synthesized. Then the GO, prGO, and prGO@cHKUST-1 membrane material was pumped onto the commercial cellulose acetate (CA) membrane by vacuum filtration, separately. The preparation detailed steps of the composite membrane were shown in Fig. 1a. In order to learn the character of each membrane and materials, scanning electron microscopy (SEM), X-ray diffraction (XRD), atomic force microscope (AFM) and other instruments were used to characterize composite membranes. The organic dye solution which include methylene blue (MB) and Congo red (CR) was used to test the separation performance of membranes. And the prGO@cHKUST-1 membrane was tested in different pH, operating time, and concentration of MB dye. Furthermore, the reusability of nanocomposite adsorbent for removal of reactive dyes was evaluated. And filtration performance towards oil-water emulsion was studied in detail. The mechanism of dyes removal and oil-water separation of the prGO@cHKUST-1 membrane was also discussed (Fig. 1b).

Morphology of HKUST-1 and orientated growth of HKUST-1 was compared. Octahedron HKUST-1 crystal with different sizes was found (Fig. S1 in Supporting information). The shape of octahedron HKUST-1 crystal is partially incomplete. But the cHKUST-1 crystal possessed a cubic crystal structure with a rough surface (Fig. 2a). In addition, no lamellar LDHs can be observed in SEM of cHKUST-1 crystal, and there's few octahedral HKUST-1 crystal almost negligible. Figs. 2b–d showed the surface morphology of the original GO, prGO, and prGO@cHKUST-1 membrane, separately. The original GO membrane exhibited a rough surface which consisted of a large number of GO layers stacked on top of each other. The prGO membrane exhibited more wrinkles than original GO membrane. The layer structure of prGO changed from flat to wavy due to the existence of topological defects and some sp^3

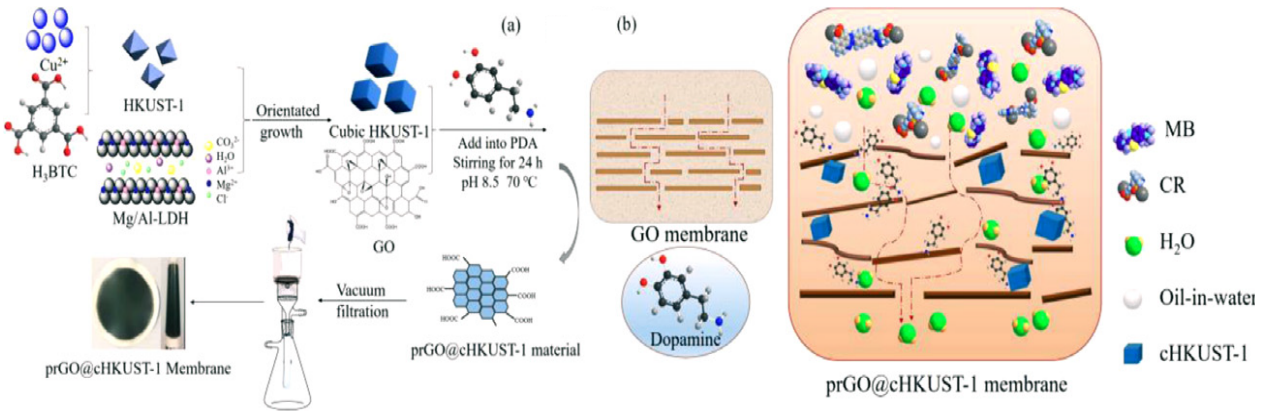

Fig. 1. (a) The preparation procedures of prGO@cHKUST-1 membranes. (b) Mechanism of dyes removal and oil-water emulsion separation by prGO@cHKUST-1 membrane.

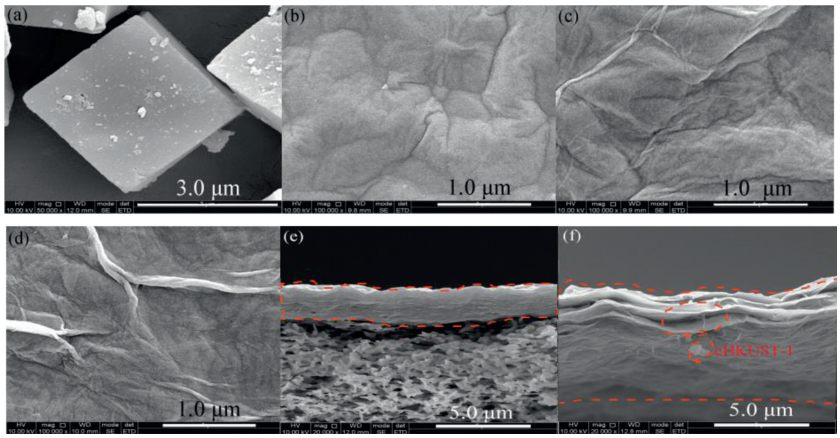

Fig. 2. SEM for cHKUST-1 crystal (a), GO (b), prGO (c), and prGO@cHKUST-1(d) membranes surface; and the cross-section morphology of prGO (e) and prGO@cHKUST-1 (f) membranes.

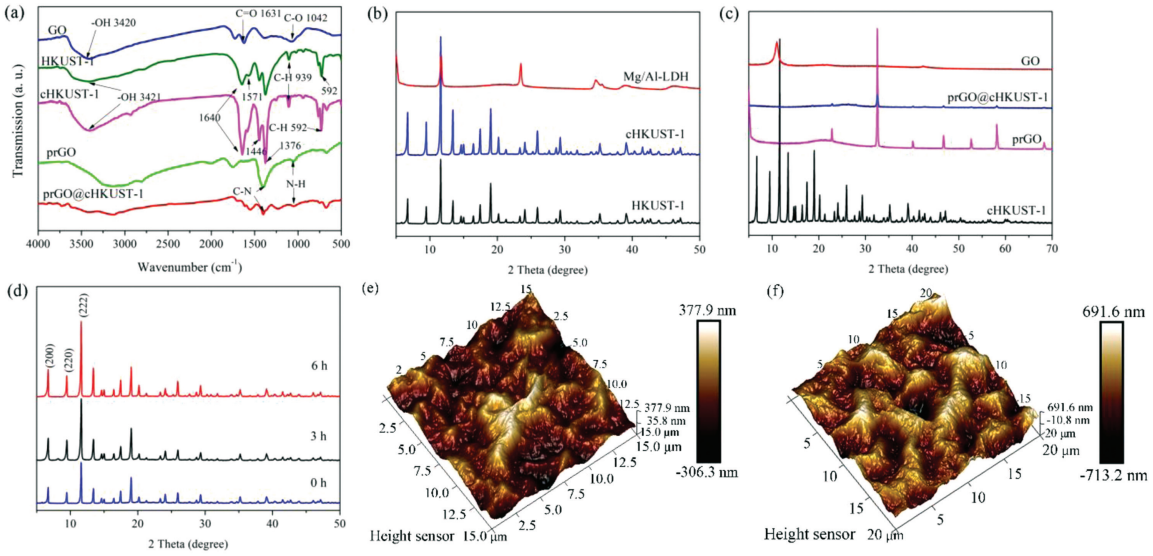

Fig. 3. FTIR spectra of GO, HKUST-1, cHKUST-1, prGO and prGO@cHKUST-1 samples (a); XRD patterns of HKUST-1, Mg/Al-LDHs, cHKUST-1 (b), prGO, GO, prGO@cHKUST-1 and cHKUST-1 samples (c), different heating duration time of cHKUST-1 (d); AFM image and roughness parameter of prGO@cHKUST-1 (e) and prGO (f) composite membranes.

hybridization of carbon atoms. And the thermal chemical reaction can let the membranes become more corrugated. The prGO@cHKUST-1 membrane has the exact same consequence. The difference between prGO@cHKUST-1 membrane and prGO membrane was cHKUST-1, and the surface of the prGO@cHKUST-1 membrane resembled a mountain peak or a valley.

From Fig. 2e, cross-section morphology of prGO showed that the stack of the membrane is relatively orderly and the layer spacing is relatively small. But for the prGO@cHKUST-1 sample, the surface flatness and smoothness of the membrane decrease, and the layer spacing of the membrane obviously increases, which are caused by the intercalation of cHKUST-1. The cHKUST-1 crystal inserted between the layers of GO (Fig. 2f), which corresponds to Fig. 1b. This may be due to the cHKUST-1 nanoparticles attached on both sides of the GO layer. Furthermore, nanoparticles attached to GO layers widen the interlayer spacing of GO and provide more active sites for water molecules to pass through [26]. In conclusion, all the phenomenon indicated that PDA can improve the microstructure of the composite membrane to increase the flux and other excellent performance. And cHKUST-1 can increase the interlayer spacing of GO. The above results are consistent with the experimental of dye removal by different composite membranes.

The bands in the Fourier transform infrared (FT-IR) spectrum can be utilized to characterize the stretching vibrations of C=O, C-O, C-H *etc.* groups. From Fig. 3a, the C-O and C=O were detected at 1631 cm^{-1} and 2921 cm^{-1}, respectively [27]. The stretching vibration of the water molecule at 3420 cm^{-1} indicates that the structure of GO has coordination water molecule [28]. Compared with the GO sample, prGO sample remains a small amount of oxygen-containing functional groups. Because full reduction of GO by thermal processes is still not achievable. The prGO sample generally has a high resemblance with GO, but with some dimension differences and structural defect [29,30]. For the HKUST-1 sample, 1112-1274 cm^{-1} was the characteristic stretching vibration peak of C=O. And the 1571, 1446, 1376 cm^{-1} were the symmetric and anti-symmetric stretching peaks of tri-benzoic acid skeleton [31]. The peaks of O-H and C-H were at 3421 cm^{-1} and 592-939 cm^{-1} [27], separately. The cHKUST-1 sample showed the same functional

groups as HKUST-1, and the intensity of the peak increased. This may indicate that oriented growth does not change the composition of functional groups, but only modifies the crystal shape of HKUST-1. For prGO and prGO@cHKUST-1 sample, the peaks at 1130 cm^{-1} was N-H group, and C-N group can be observed at 1403 cm^{-1}. According to the literature, these two bonds come from dopamine [32]. In addition, the characteristic peaks of $-CH_2$, R-NH_2 and C=C of dopamine were also found at 2926, 3400, 1600 cm^{-1}, separately. Compared with prGO sample, the C-N peak strength of prGO@cHKUST-1 sample decreased. Nonetheless, the absorption peaks of the composite membrane sample which associated with oxygen-containing functional groups weaken or disappear, indicating the GO was reduced by PDA. Notably, the adsorption peaks of prGO@cHKUST-1 sample move to another wavenumber compared with pristine GO and cHKUST-1, which demonstrated that prGO@cHKUST-1 was successfully synthesized as a composite membrane rather than simply a mechanical mixture.

The XRD showed the crystal structure changes before and after orientated growth of the HKUST-1 (Fig. 3b). It is obvious that the cHKUST-1 retained the characteristic diffraction peaks of original material. Diffraction peaks of Mg/Al-LDHs adsorbent are at 2θ of 11.72°, 23.58°, 34.99°, 39.56°, and 47.10°, respectively. And the diffraction peaks correspond to (003), (006), (009), (015) and (018) crystal facets, respectively. Among them, the diffraction peaks corresponding to (003) and (006) crystal facets are quite strong, while the other peaks are relatively weak, indicating that the crystal grows along the central axis [33,34]. HKUST-1 has several characteristic peaks of 2θ at 6.71°, 9.48°, and 13.42°, corresponding to (200), (220) and (400) crystal facets, respectively [35]. The Fig. 3c showed the typical XRD patterns at 2θ of around 10.2° of GO. The prGO and prGO@cHKUST-1 sample had hardly found this characteristic peak, which illustrated that the oxygen-containing groups of GO decreased by PDA [36]. After adding cHKUST-1 to modify the prGO@cHKUST-1 composite membrane, the number of diffraction peaks of GO and cHKUST-1 decreased. Those indicated that the crystals get distorted during the synthesis of the membrane, probably due to contortions at the contact points between GO and cHKUST-1.

To identify the orientated growth mechanism of HKUST-1, XRD characteristic of different time periods of synthesis was measured. From Fig. 3d, the change of absorption peak intensity of HKUST-1 crystal growing from octahedron to cube can be observed. This phenomenon can be attributed to surface energy. The crystal shape is determined by the growth rates of the specific facets. The surface energy of {100} is larger than that of the {111} [37]. According to the literature, octahedron has eight {111} crystal faces, which have the most stable structure [38]. When the LDHs were added in, the Al ions might compete with Cu ions and connect with BTC ligands, resulting in the appearance of high-energy surfaces {100} [39]. This restricted the growth of crystals towards stable octahedron to some extent. As the hydrothermal reaction proceeds, an increasing number of Al ions compete with Cu ions. Overall, the increase intensity of (200) and (400) can certify the orientated growth of {100}.

The AFM was also used to characterize the morphology of membranes. The dark regions represent the valley or membrane hole, and the light part indicated the bulge part of the membrane [37]. Bulge part of the prGO@cHKUST-1 sample might be caused by cHKUST-1 inserting into the GO interlayers, and constructing a hierarchical composite nanoscale material (Fig. 3e). Furthermore, compared with prGO sample (Ra =75.5 nm) in Fig. 3f, the average roughness (Ra) of prGO@cHKUST-1 sample was 167.1 nm, which indicated the increase of the roughness. The reduced oxygen-containing functional groups of GO, and accumulation of cHKUST-1

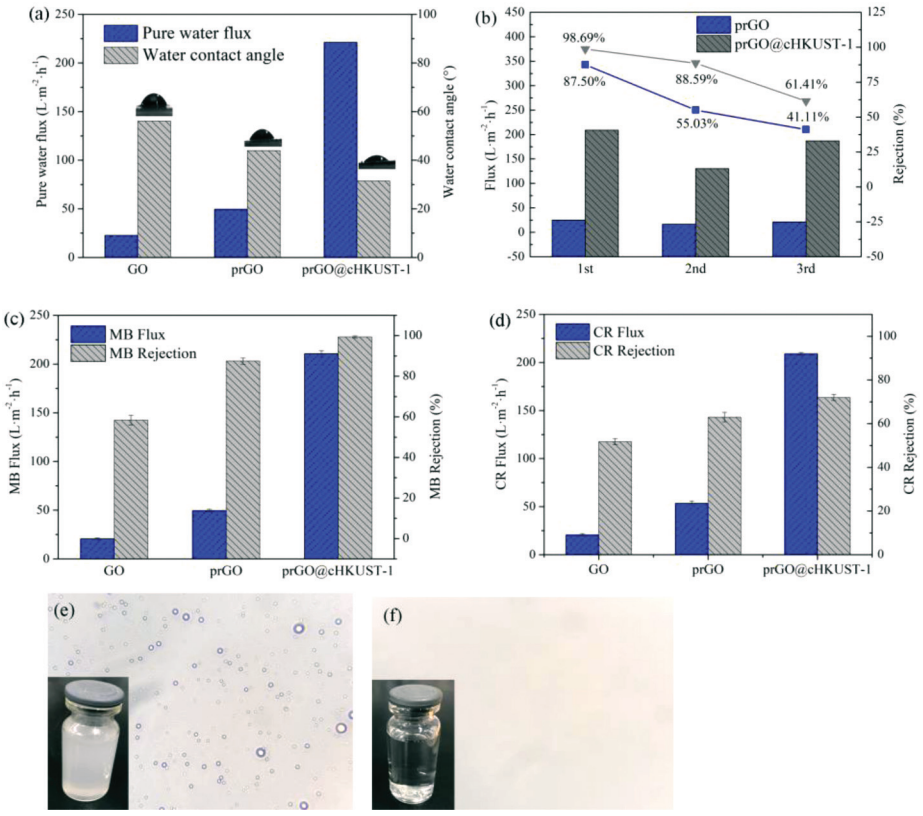

Fig. 4. The water contact angle of different membranes (a); the MB flux and rejection of prGO and prGO@cHKUST-1 membranes in three cycles (b); the flux and rejection of membranes for MB (c) and CR (d); the separation of oil-water emulsion before (e) and after (f) treatment by electron microscope.

materials on the membrane surface, which leading to the flatness of the membrane increases. Moreover, surface topologies of composite membranes were distorted in the thermal synthesis process, resulting in pore channels on the membrane surface. All those reasons give birth to the roughness of the prGO@cHKUST-1 membrane.

In order to verify the wettability of membranes, water contact angle (WCA) was measured. While the water dropped onto different membrane surfaces, contact angle increased with the increase of membrane hydrophobicity. From Fig. 4a, the WCA of original GO, prGO, and prGO@cHKUST-1 composite membrane is 56.16°, 43.99° and 31.50°, respectively. According to our previous study, the flux and WCA of GO membrane modified by HKUST-1 are about 100 ($L\,m^{-2}\,h^{-1}$) and 45° [27]. This further illustrates that cHKUST-1 can improve the performance of the composite membrane. The prGO@cHKUST-1 membrane has excellent hydrophilicity and ultrahigh flux (210.7 $L\,m^{-2}\,h^{-1}$), which had the same order of magnitude as the properties of ultrahigh flux of membranes by previous studies [40]. The excellent property could be accounted for the following aspects. Firstly, the composite membrane which exhibited an excellent hydrophilic surface provides a fast channel for the pass through of water molecules [41]. Secondly, under the effect of ultrasound and PDA reduction, the flatly stacked GO layer was corrugated, or even fractured. Therefore, the fuzzy pores was formed on the surface of composite membrane [42]. These fuzzy pores provide a channel for molecules, which causing an increased membrane flux after reduction. Thirdly, the cHKUST-1 insert into GO inter-layer to increase the layer spacing of membrane, and let the resistance of water molecules passing through the membrane decreased [43]. For prGO membrane, there is not any significant increase in layer spacing (Fig. 2e). The roughness is linked to the effective filtration area, and roughness is proportional to effective filtration area [44]. In this way, the modified membrane has excellent rejection property than the original membrane. This contact angle test can be inferred the hydrophilic membrane (prGO@cHKUST-1) has higher flux.

Generally, recyclability is an essential indicator for examining membrane performance. From Fig. 4b, the prGO@cHKUST-1 membrane can maintain a high flux. After three times of test, the rejection of dye by the membrane showed a slow-lowing trend. While the dye molecules pass through the membrane, they may occupy the active sites on the membrane surface or blocked by smaller pore sizes. After the flux of pure water test, the membranes expanded spontaneously in water, resulting the second flux and rejection of MB decreased. And the hydration of oxygen-containing groups on the prGO layers with water molecules which are expected to result in the flux of membranes is unstable. Improved membranes have a strong rejection on MB (> 99%) and CR (> 68%) (Figs. 4c and d). The effect of the CA membrane on the flux of the composite membrane can be ignored. The decreased rejection of CA membrane to high concentration dye is one of the reasons that the decreased rejection of composite membrane. (Fig. S2 in Supporting information). Flux of prGO@cHKUST-1 membrane is 10 times higher than pure GO membrane, and the rejection of CR is approximately equal to prGO membrane, but has great differences in dye flux. Therefore, the addition of cHKUST-1 and reduction effect of PDA can enhance the permeability to improve rejection performance.

The mechanism of dye rejection and oil-water emulsion separation by the membranes is shown in Fig. 1b, which is closely associated ions electronegativity, physical sieving, adsorption, and intermolecular forces [45]. Due to the strong interaction between adjacent nanosheets, GO nanosheets are stacked in parallel and stacked together, which obstructs the transport of water molecules, and the narrowing of interlayer space is not conducive to the increase of water flux [46]. With the reduction effect of PDA, the GO nanosheets bended and piled up in waves [47]. Moreover, the cHKUST-1 with stable property and large surface area inserted into GO interlayer and attached to both sides of the layer. On the one hand, it can increase the layer spacing of GO nanosheets [48]. On the other hand, it can provide roughness and more active sites on the membrane surface. In consequence, the irregular GO lamellar arrangement and cHKUST-1 intercalation provide a fast and effective channel for the passage of water molecules [42]. In addition, the prGO@cHKUST-1 membrane has a larger specific surface area and more active sites, which can improve the adsorption performance. The rough surface enhanced the hydrophilicity and effective filtration area of the membrane. The increased hydrophilicity provides a strong impetus for the separation of solvent and solute [49]. Strong hydrophilicity makes solute trapped on the membrane, and the driving force is mainly the affinity attraction of solid on the membrane surface of solute, and the repulsive force of solvent with hydrophobic material. Moreover, the fuzzy pores on the membrane surface can achieve physical screening to prevent macromolecular pollutants from passing through the membrane. Electrostatic interaction between the membrane surface and dye molecules can promote or inhibit the penetration and adsorption of dye molecules. Under these combined effects, the prGO@cHKUST-1 membrane achieves efficient purification of dyes and oil-water emulsions.

In order to investigate the influence of different experience condition, the different concentration and pH of MB and CR on prGO@cHKUST-1 composite membrane was tested. As MB concentration varied from 20 mg/L to 100 mg/L, the flux was from 214.7 $L\,m^{-2}\,h^{-1}$ to 179.6 $L\,m^{-2}\,h^{-1}$, while the rejection decreased from 99.5% to 58.4% (Fig. S3 in Supporting information). The same phenomenon was found in different concentration of CR experiments, but the variation trend is even greater than MB. With the increase of dye concentration, the membrane can only retain part of the dye molecules, while other dye molecules can pass through the membrane material, so that the rejection rate of dye by the membrane is reduced. In addition, the removal of dye by the prGO@cHKUST-1 membrane is mainly based on adsorption, supplemented by interception and electrostatic action. Different pH values have a significant effect on MB flux and have little effect on MB rejection. MB flux increased quickly from 146.3 $L\,m^{-2}\,h^{-1}$ to 214.7 $L\,m^{-2}\,h^{-1}$ in the pH value of 3-7 (Fig. S4 in Supporting information). In the pH value of 7 and 9, MB flux remains at a relatively higher value, and then decreased at the pH value of 11. When the pH changes from 3 to 11, the MB rejection can retain about 99.5%. For rejection test for CR, the pH has an obvious effect on flux and rejection. The influence of pH on CR flux has increases from pH 3 to 7, and tends to be stable after pH value of 7. The change of pH value of the solution affects the structure of dye molecules in solution and the surface charge of the membrane, promoting or inhibiting the permeation rate and adsorption rate of dye molecules on the membrane surface. Moreover, the long-time experiment showed that prGO@cHKUST-1 membrane exhibited higher flux stability than the prGO membrane (Fig. S5 in Supporting information), which further proved that the membrane with high water flux also has superior dye flux.

The prGO@cHKUST-1 membrane also has excellent separation property for oil-water emulsion. By comparison (Figs. 4e and f), oil drops were not found in Fig. 4f, which indicated that the membrane has an excellent effect on separating oil-water emulsion. Moreover, the flux of the prGO and prGO@cHKUST-1 membrane was 9.2 $L\,m^{-2}\,h^{-1}$ and 28.6 $L\,m^{-2}\,h^{-1}$, respectively, and the rejection were both about 99.6%. The membrane which modified by cHKUST-1 has higher flux than prGO membrane. In the initial stage of the oil-water separation experiment, the water flux is larger. At long time, the machine oil emulsion accumulated on the surface of the membrane and blocked the pores. The flux

declined with the increase of mass transfer resistance. Compared with composite membranes (Table S1 in Supporting information), our composite membrane has excellent dye rejection and oil-water emulsion separation performances.

In summary, we successfully prepared hydrophilic and anti-fouling prGO@cHKUST-1 composite membrane for dye molecules and oil-water emulsion separations. The characterization of SEM, FTIR, XRD, and AFM confirmed the synthesis of prGO, cHKUST-1, and prGO@cHKUST-1 sample. The prGO which was partially reduced by PDA increased the inter-layer spacing by the intercalation of cHKUST-1. Benefiting from the larger pores and stability of cHKUST-1, the prGO@cHKUST-1 composite membrane has a high rejection for MB (99.5%) and CR (71.2%) with a maximum flux ($\sim$210 L m^{-2} h^{-1}). And excellent oil-water emulsion separation performance was also found. Overall, the prGO@cHKUST-1 membrane can remain stable under long-time reaction. Oriented growth of MOFs provided an instructive approach to obtain special functional materials, and enhance the adsorption, rejection, catalysis and stability performance of GO based composite membrane.

Declaration of competing interest

The authors declare that they have no known competing financial interests or personal relationships that could have appeared to influence the work reported in this paper.

Acknowledgments

This work was financially supported by key projects of science and technology of Science & Technology Department of Sichuan Province (No. 2018GZ0421). In addition, we especially wish to thank “ceshigo research service platform” (www.ceshigo.com) whose support has given our article.

Appendix A. Supplementary data

Supplementary material related to this article can be found, in the online version, at doi:https://doi.org/10.1016/j.cclet.2020.04.011.

References

[1] M. Chen, Y. Ding, Y. Liu, et al., Pet. Sci. Technol. 36 (2018) 141–147.
[2] X. Zhang, H. Li, J. Wang, et al., J. Membr. Sci. 581 (2019) 321–330.
[3] Y. Gao, K. Su, X. Wang, Z. Li, J. Membr. Sci. 574 (2019) 55–64.
[4] Y. Zheng, B. Cheng, W. You, et al., J. Hazard. Mater. 369 (2019) 214–225.
[5] S. Vahidhabanu, A.A. Idowu, D. Karuppasamy, et al., ACS Sustain. Chem. Eng. 5 (2017) 10361–10370.
[6] J. Sun, H. Bi, S. Su, et al., J. Membr. Sci. 553 (2018) 131–138.
[7] S.A. Hosseini, M. Vossoughi, N.M. Mahmoodi, M. Sadrzadeh, J. Clean. Prod. 183 (2018) 1197–1206.
[8] J.H. Jhaveri, Z.V.P. Murthy, Desalination 379 (2016) 137–154.
[9] C. Zhou, J. Cheng, K. Hou, et al., Chem. Eng. J. 301 (2016) 249–256.
[10] W. Li, X. Yang, H. Fu, et al., J. Nanosci. Nanotechno. 19 (2019) 7089–7096.
[11] T. Ouyang, J. Tang, F. Liu, C.T. Chang, J. Nanosci. Nanotechno. 19 (2019) 7035–7043.
[12] X. Wan, Y. Zhan, Z. Long, et al., Chem. Eng. J. 330 (2017) 491–504.
[13] D. Vikraman, S. Thiagarajan, K. Karuppasamy, et al., Appl. Surf. Sci. 479 (2019) 167–176.
[14] B.B. Wang, X.X. Zhong, B.M. Ming, et al., Appl. Surf. Sci. 480 (2019) 1054–1062.
[15] F. Li, Z. Yu, H. Shi, et al., Chem. Eng. J. 322 (2017) 33–45.
[16] A. Karkooti, A.Z. Yazdi, P. Chen, et al., J. Membr. Sci. 560 (2018) 97–107.
[17] J. Zhang, X. Pan, Q. Xue, et al., J. Membr. Sci. 532 (2017) 38–46.
[18] A. Chakraborty, H. Acharya, Colloid Interfac. Sci. 24 (2018) 35–39.
[19] T.A. Makhetha, R.M. Moutloali, J. Membr. Sci. 554 (2018) 195–210.
[20] J. Yu, Y. Yang, M. Wei, Acta Chim. Sinica 77 (2019) 1129–1139.
[21] B. Song, Z. Zeng, G. Zeng, et al., Adv. Colloid Interface Sci. 272 (2019) 101999.
[22] Z.L. Cheng, Y.Y. Liu, B.C. Cao, Mater. Lett. 175 (2016) 215–218.
[23] Z. Li, M. Shao, L. Zhou, et al., Adv. Mater. 28 (2016) 2337–2344.
[24] J. Wang, J. Tang, B. Ding, et al., Small 14 (2018) 1704461.
[25] H.R. Cho, Y.M. Kwon, Y.J. Lee, et al., Appl. Clay Sci. 156 (2018) 187–194.
[26] D. Guo, X. Song, L. Tan, et al., Chem. Eng. J. 356 (2019) 955–963.
[27] Y. Liu, M. Zhu, M. Chen, et al., Chem. Eng. J. 359 (2019) 47–57.
[28] Y. Liu, W. Tu, M. Chen, et al., Chem. Eng. J. 336 (2018) 263–277.
[29] D.R. Dreyer, S. Park, C.W. Bielawski, R.S. Ruoff, Chem. Soc. Rev. 39 (2010) 228–240.
[30] Y. Shang, D. Zhang, Y. Liu, C. Guo, Bull. Mater. Sci. 38 (2015) 7–12.
[31] X. Cui, X. Sun, L. Liu, et al., Chem. Eng. J. 369 (2019) 898–907.
[32] L. Li, B. Li, J. Zhang, et al., J. Mater Chem A. 4 (2016) 512–518.
[33] W. Zhang, N. Li, Z. Xie, et al., Int. J. Hydrogen Energy. 44 (2019) 21858–21864.
[34] E.R. soliman, Y.H. Kotp, E.R. Souaya, et al., Compos. Part B: Eng. 175 (2019) 107131.
[35] H. Xia, Z. Li, X. Zhong, et al., Chem. Eng. Sci. 203 (2019) 43–53.
[36] C. Petit, T.J. Bandosz, J. Colloid Interface Sci. 447 (2015) 139–151.
[37] P. Li, W. Wu, J. Liu, et al., J. Membr. Sci. 555 (2018) 327–336.
[38] Z. Wang, L. Ge, M. Li, et al., Chem. Eng. J. 357 (2019) 320–327.
[39] X. Fang, J. Li, X. Li, et al., Chem. Eng. J. 314 (2017) 38–49.
[40] Y. Ren, T. Li, W. Zhang, et al., J. Hazard Mater. 365 (2019) 312–321.
[41] A. Rahimpour, M. Jahanshahi, S. Khalili, et al., Desalination 286 (2012) 99–107.
[42] L. Qiu, X. Zhang, W. Yang, et al., Chem. Commun. 47 (2011) 5810–5812.
[43] J. Ma, X. Guo, Y. Ying, et al., Chem. Eng. J. 313 (2017) 890–898.
[44] H. Sun, B. Tang, P. Wu, ACS Appl. Mater. Interfaces 9 (2017) 21473–21484.
[45] A.T. Smith, A.M. LaChance, S. Zeng, et al., Nano Mater. Sci. 1 (2019) 31–47.
[46] X. Wu, Y. Wu, L. Chen, et al., J. Membr. Sci. 553 (2018) 151–162.
[47] J.J. Lu, Y.H. Gu, Y. Chen, et al., Sep. Purif. Technol. 210 (2019) 737–745.
[48] M.S. Rahmanifar, H. Hesari, A. Noori, et al., Electrochim. Acta 275 (2018) 76–86.
[49] R.R. Nair, H.A. Wu, P.N. Jayaram, et al., Science 335 (2012) 442–444.